



Nineteenth Australasian Wind Engineering  
Society Workshop, April 4-6, 2018,  
Torquay, Victoria

## Wind Fragility Assessment for Metal Roof Damage in Non-cyclonic Regions of Australia

Hao Qin<sup>1</sup>, Mark G. Stewart<sup>2</sup>

<sup>1</sup>*School of Engineering, The University of Newcastle, NSW2308, Australia*

*Email: hao.qin@uon.edu.au*

<sup>2</sup>*Centre for Infrastructure Performance and Reliability, The University of Newcastle, NSW2308, Australia.*

*Email: mark.stewart@newcastle.edu.au*

### ABSTRACT

Metal roof sheeting is one of the most vulnerable housing components under high wind uplift pressure. A fragility assessment for roof sheeting loss facilitates the risk assessment and mitigation for housing subjected to extreme wind loading. This paper aims to develop a reliability-based fragility methodology for metal roofing of a representative Australian contemporary house subjected to non-cyclonic extreme wind loading. The fragility analysis considers roof sheeting loss due to overloading of cladding-to-batten and batten-to-truss connections. A Monte Carlo Simulation in conjunction with a finite element approach are proposed to carry out the wind fragility assessment for the entire roof envelope. It was found that, for a 500-year wind speed, the mean roof sheeting loss is negligible for the representative contemporary housing built in Melbourne, whereas considerable roof damage is predicted for those built in Brisbane when subjected to windward wall dominant openings.

### 1. Introduction

Metal roof sheeting has been widely used in Australian residential construction, which is typically the most vulnerable component of timber-frame houses under high wind loads. The disengagement of metal sheets from roof structure may cause significant damage to building interiors and contents by allowing for rainwater intrusion. Metal roof sheets subjected to wind uplift pressure are often damaged by detaching from battens and/or separating from rafter/truss with battens attached. These two types of roof sheeting loss are predominantly attributed to the overloading of cladding-to-batten and batten-to-rafter/truss connections, respectively (Henderson and Ginger 2007).

A wind fragility function typically expresses the damage state as a function of wind speed, which offers a convenient and effective metric to forecast the extent of wind damage. Most fragility methodologies developed for metal roof sheeting loss (e.g. Henderson and Ginger 2007; Sivapathasundaram and Mahendran 2016; Ji *et al.* 2018) only considered the probabilities of 'first failure' of connections. However, the load redistribution to neighbouring connections beyond the first failure and the consequent progressive failure were not explicitly examined by these studies, and therefore the redundancy of metal roof sheets could be somewhat underestimated.

This paper develops a reliability-based fragility methodology to predict the damage progression of corrugated metal roof sheeting on Australian contemporary housing under non-cyclonic extreme wind loading. The fragility analysis considers roof sheeting loss due to overloading of cladding-to-batten and batten-to-truss connections. A Monte Carlo Simulation (MCS) in conjunction with a finite element approach were proposed to carry out the wind fragility assessment for the entire roof envelope, which enables the stochastic modelling of load redistribution and failure progression of roof connections under spatially varying wind uplift pressure. The developed fragility methodology was illustrated on representative contemporary housing built in the suburbs of Melbourne and Brisbane.

## 2. Reliability-based Fragility Methodology

The fragility of a structural component or system is typically defined as the probability of damage state  $DS$  conditional on a given hazard  $H$ . The damage state herein is measured by the proportion of roof sheeting loss and the hazard is gust wind speed. The wind fragility is therefore the extent of roof sheeting loss  $R_{loss}$  at a given gust wind speed  $v$ , which is expressed as

$$\Pr(DS|H) = \Pr[DS = R_{loss}|H = v] \quad (1)$$

This study considers roof sheeting loss due to overloading of cladding-to-batten and batten-to-truss/rafter connections. The loss of a single roof sheet is assumed to occur when a critical number of cladding fasteners fail as inadequate fixings may lead to loss of functionality, stability and integrity of the roof sheet. The failure of a single cladding-to-batten or batten-to-truss/rafter connection is governed by the following limit state function

$$g = R - (W - D_L) \quad (2)$$

where  $R$  represents the resistance of the considered connection against pull-out and pull-over failure, and  $W$  is the wind uplift load acting on this connection.  $D_L$  is the dead load arising from the weight of steel battens and metal roof sheets. A connection fails if  $g \leq 0$ . In this study, the uplift loads acting on roof connections are obtained by using a finite element analysis (FEA), which takes into account the load sharing and redistribution among connections under the spatially varying wind uplift pressure. The dead load is considered as deterministic in the finite element modeling by specifying the density of metal roof sheets and steel battens. The details of the finite element modeling are described in Section 4.

The failure of a single roof sheet occurs when the number of failed fasteners on the roof sheet  $N_f$  exceeds the critical number of failed fasteners causing the sheet loss,  $N_{cr}$ .  $N_{cr}$  is equivalent to the sheet failure criterion (SFC) defined in Stewart *et al.* (2017). Note that the failure of batten-to-rafter/truss connections leads to load redistribution in other connections and cladding fasteners attached to a batten are assumed to fail when the batten detaches from rafter/truss. A triangular probability distribution proposed in Stewart *et al.* (2017) is employed here to model  $N_{cr}$ . The lower and upper bound for  $N_{cr}$  are 10% and 80% of the total number of fasteners on a single sheet, respectively. For more details of the triangular distribution model of  $N_{cr}$ , see Stewart *et al.* (2017).

The assessment of  $N_f$  requires the fragility model to account for progressive failure of roof connections. An event-based MCS in conjunction with the FEA approach were employed in this study to evaluate the wind fragility for roof envelope. In each run of MCS, the spatially distributed wind pressures and structural resistances of roof connections are randomly generated as the input to the finite element model of the entire roof envelope. The wind uplift loads acting on roof connections are then obtained from the FEA. Both the overloaded cladding-to-batten and batten-to-truss/rafter connections are removed from the finite element model, and the FEA is further conducted to evaluate the load redistribution and failure progression. For each wind speed, the loss of a roof sheet is deemed to occur if  $N_f \geq N_{cr}$ . The MCS and FEA approach proposed in the present study enables the developed fragility curves to relate the extent of roof sheeting damage with gust wind speeds.

The fragility assessment methodology proposed in the present study is illustrated on representative contemporary housing built in the suburbs of Melbourne and Brisbane. The dimension, shape and construction type of the representative house were determined by field surveys completed by the Cyclone Testing Station (CTS) at James Cook University (JCU) (Parackal *et al.* 2016). Figure 1 shows the representative one-story house. It is a timber-frame construction with a 21.5° timber roof truss at 600 mm spacings on a complex hip-end roof. Roof cladding is corrugated metal sheeting attached to metal top-hat battens using screw fasteners at 900 mm spacings. More details of the representative contemporary house can be found in Parackal *et al.* (2016).

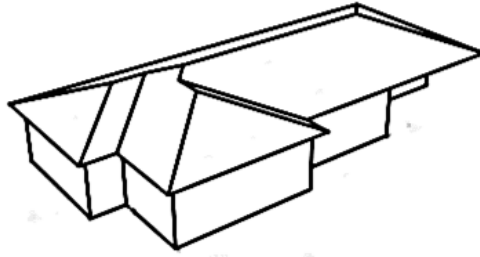


Fig. 1. One-story representative contemporary house

### 3. Probabilistic Modeling of Wind Loading and Resistance

The wind uplift pressure ( $P_U$ ) acting on the roof envelope is modelled probabilistically as (Holmes 1985; Stewart *et al.* 2017)

$$P_U = \lambda \cdot (C \cdot T \cdot E^2 \cdot D^2 \cdot G \cdot \frac{\rho_{air}}{2}) \cdot v^2 \quad (3)$$

where  $v$  is the maximum 0.2 second gust velocity at 10m height in open terrain;  $\lambda$  is a factor accounting for wind loading modeling uncertainties;  $C$  is the quasi-steady pressure coefficient that is a combination of external ( $C_{pe}$ ) and internal pressure coefficient ( $C_{pi}$ );  $T$  is the shielding factor;  $E$  is a terrain height multiplier that accounts for the exposure and height of the building considered;  $D$  is a factor accounting for wind directionality effects;  $G$  is a factor that accounts for gusting effects, and  $\rho_{air}$  is the air density. These parameters, except for  $C$ , are assumed to follow a lognormal distribution. The means and coefficient of variations (COV) for these parameters presented in Stewart *et al.* (2017) are used in this study. The nominal values for these parameters are obtained from Standards Australia (2011) for suburban housing below 10m height with no shielding. Nominal values of  $D$  could vary depending on wind directions at various sites to account for the wind directionality effect.  $\lambda$ ,  $T$ ,  $E$ ,  $D$ ,  $G$  and  $\rho_{air}$  are assumed to be fully correlated for all areas of the roof envelope.

Wind tunnel testing was employed in this study to evaluate the external pressure coefficients in Eq. (3). The spatially and temporarily varying external pressure coefficients for the roof surface were measured in a wind tunnel test conducted in the Boundary Layer Wind Tunnel at JCU. The peak external pressure coefficients at a total of 320 pressure tap locations for each wind direction were modelled by a Gumbel probability distribution with the scale and location parameters estimated using a maximum likelihood method based on the wind tunnel observations. More details about the wind tunnel test can be found in Parackal *et al.* (2016) and Stewart *et al.* (2017).

The failure of windows, doors and roof sheets during an extreme wind event may change the internal pressure and therefore affect the roof damage assessment. In this paper, two typical scenarios are assumed for the internal pressure evaluation, namely, dominant openings existing on the windward wall and effectively sealed building without any wall openings. Both of the two scenarios consider the increasing roof openings due to damage progression of roof sheeting. The internal pressure coefficient is assumed to follow a normal distribution with a COV of 0.33 (e.g. Sivapathasundaram and Mahendran 2016). For the later scenario, the mean internal pressure coefficients would equal to the average of external pressure coefficients at roof openings. Derived from the mass conservation theory (Holmes 2015), the mean internal pressure coefficient for the former scenario is calculated as

$$C_{pi} = \frac{C_{PW}}{1 + (\frac{A_R}{A_W})^2} + \frac{C_{PR}}{1 + (\frac{A_W}{A_R})^2} \quad (4)$$

where  $C_{PW}$  is the average of external pressure coefficients at windward wall openings and  $C_{PR}$  is the average of external pressure coefficients at roof openings;  $A_W$  is the total size of wall openings and  $A_R$  is the total size of roof openings. Note that only roof openings due to the damage progression of metal sheets are considered in this study (i.e. ignoring possible effect of flashings, vents, etc). The approximate trend of  $C_{pi}$  change with increasing  $A_R/A_W$  for the windward wall dominant opening

scenario is depicted in Figure 2. The figure implies that the adverse effect of internal pressure is relieved with increasing roof sheeting loss.

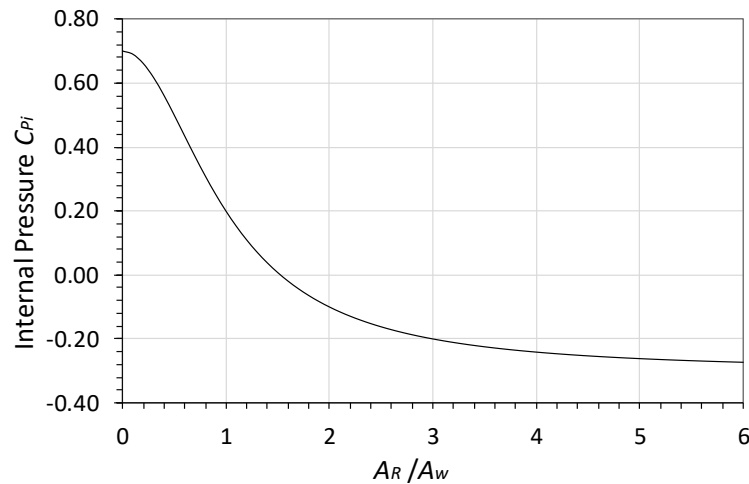


Fig. 2. Internal pressure evolution with increasing roof sheeting loss

The pull-over and pull-out failure were considered as the failure modes for cladding-to-batten and batten-to-rafter/truss connections. A lognormal distribution was used to model both the pull-over and pull-out capacities (e.g. Henderson and Ginger 2007) for roof connections with the mean and COV estimated from the test data in literature. Refer to Stewart *et al.* (2017) for more details about the statistical parameters for the connection resistances.

#### 4. Finite Element Analysis (FEA) for Fastener Loads

A FEA approach is presented in this section to evaluate the wind uplift loads acting on roof connections and the load redistribution after the failure of one or more fasteners. Commercial FEA software ANSYS was employed to model the entire roof envelope including corrugated metal roof sheeting, steel roof battens, cladding-to-batten and batten-to-truss/rafter connections. Four-node quadrilateral shell elements including both bending and membrane stiffness were used to model the corrugated metal sheet with six degrees of freedom at each node. The roof envelope layout and a typical corrugated metal roof sheet in the finite element modeling are depicted in Figure 3. The typical corrugated metal sheet on the roof has five spans and each span has a length of 900 mm. The sheet has a width of 762 mm, base metal thickness of 0.42 mm and crest height of 22 mm. Roof sheets with other shapes were configured by trimming the typical sheets at ridgelines and hips.

The proposed FEA approach is mainly aimed at evaluating the wind uplift forces in roof connections, which in conjunction with the sampled connection resistances are used to assess the overloading of fasteners in a MCS. To this end, localized dimpling, buckling and fracture of the metal roof sheet were not considered in the proposed FEA approach. In addition, according to Mahendran (1994), the majority of the corrugated metal sheeting are still in elastic range when the fasteners fail. Thus, the material properties for the corrugated metal sheets were assumed to be isotropic and linear-elastic. Two-node beam elements were used to model the steel roof battens under the corrugated metal roof sheeting with material and section properties obtained from manufacture's specifications (Lysaght 2014). The cladding-to-batten and batten-to-truss/rafter connections were approximately modelled by linear spring elements. The roof trusses were not modelled and pinned supports were assumed to represent the attachment points of batten fasteners to rafters. In each MCS realisation, the reaction forces of the spring elements obtained from a static FEA are compared with the sampled resistances of roof connections according to Eq. (2), and overloaded connections are then removed from the finite element model for further analysis of progressive failure.

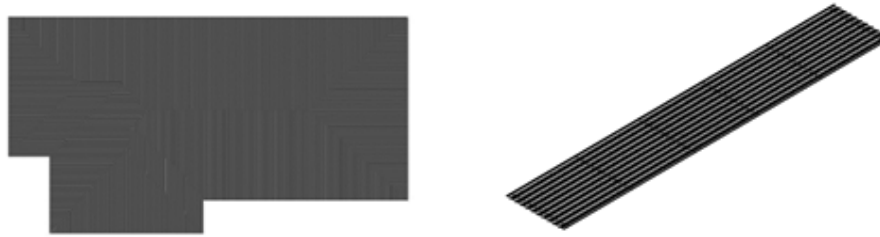


Fig. 3. Roof envelope layout and a five-span corrugated metal roof sheet in the finite element modeling

## 5. Results of Fragility Analysis

A fragility analysis was carried out for the representative house at suburbs of Brisbane and Melbourne using the proposed MCS and FEA methodologies. The fragilities were calculated up to gust wind speed of 80 m/s considering two wall opening scenarios as described in Section 3. Random wind direction and building orientation were taken into account for the fragility analysis by utilizing the wind directional multipliers given in Standards Australia (2011) for  $D$  in Eq. (3). The fragility curves for the representative house built in Brisbane and Melbourne considering random building orientation and wind direction are depicted in Figure 4. The figure shows that the fragility curves for the representative house in Brisbane are higher than those for Melbourne house. This is expected because the maximum gust wind speed is likely to appear in any wind direction of Brisbane but only a few prevailing wind directions of Melbourne. The maximum gust wind speed corresponding to a 500-year return period for Brisbane is 57 m/s (Standards Australia 2011). At this wind speed, the mean roof sheeting loss for the representative house in Brisbane is 4.14% for the windward wall dominant opening scenario and 0.10% for the scenario without wall dominant openings. While the latter loss is insignificant, the former may result in a considerable economic loss, for example, roughly 15% of the total building and contents value as inferred from Stewart (2016). The mean roof sheeting loss for the representative house in Melbourne at the 500-year gust wind speed, i.e. 45 m/s (Standards Australia 2011), are negligible for both scenarios (i.e. with and without wall dominant openings). The progressive failure of fasteners for four selected roof sheets (i.e. A1, A2, B1 and B2) with increasing wind speed in one MCS realisation for a wind attack angle of  $180^\circ$  is shown in Figure 5, which implies that the ‘first failure’ may not necessarily lead to a cascading failure. First failed fastener that initiates at a relatively higher wind speed is more likely to result in a rapid failure progression of connections.

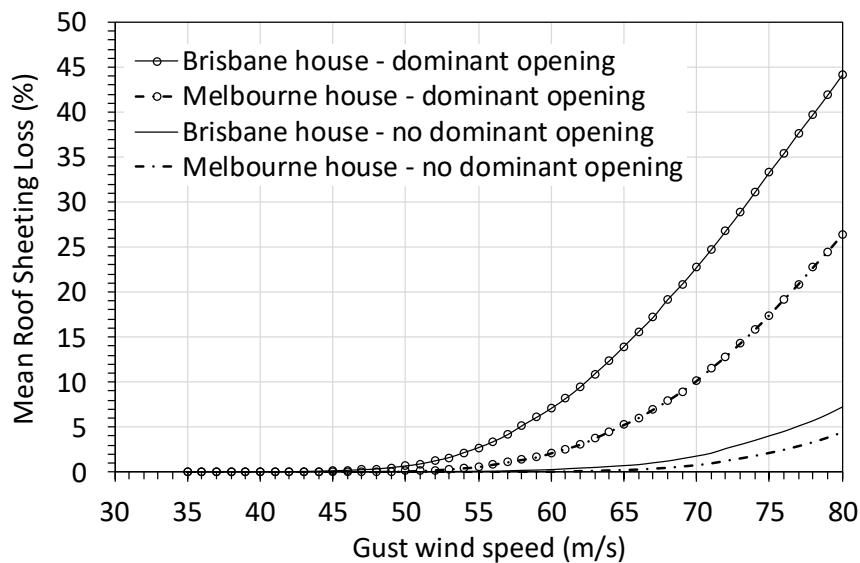


Fig. 4. Fragility curves for the representative contemporary house

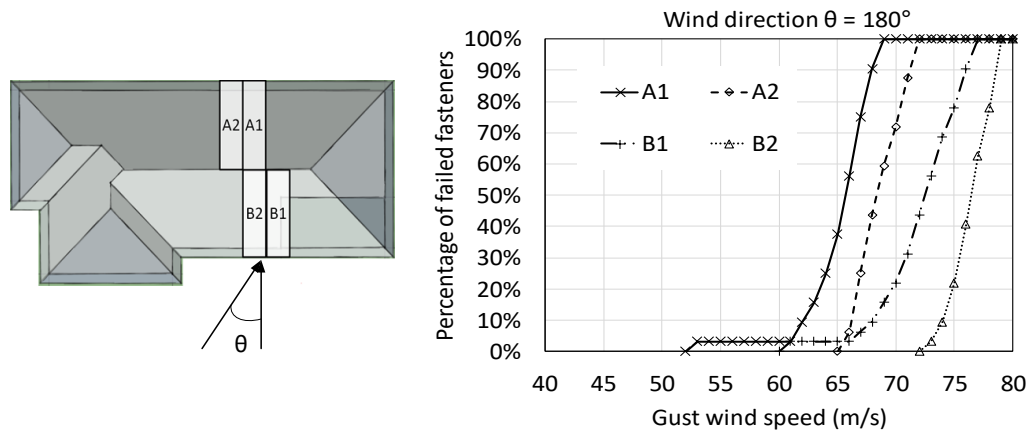


Fig. 5. Progressive failure of fasteners for four selected roof sheets in one MCS realisation

## 6. Conclusions

This paper describes the development of a reliability-based fragility methodology to evaluate the metal roof sheeting loss for Australian contemporary housing under wind uplift pressure. An event-based MCS in conjunction with a FEA approach were proposed to carry out the wind fragility assessment for the entire roof envelope, which enables the stochastic characterisation of spatially varying wind uplift pressure and failure progression of roof connections. The proposed fragility methodology was illustrated on representative contemporary housing built in Brisbane and Melbourne. It was found that, if no windward wall dominant opening exists, the mean roof damage is negligible under the gust wind speed corresponding to a 500-year return period for the representative house in both Brisbane and Melbourne. When subjected to windward wall dominant openings, considerable roof damage is predicted at the 500-year wind speed for the representative house built in Brisbane.

## References

- Henderson, D. J., & Ginger, J. D. (2007). Vulnerability model of an Australian high-set house subjected to cyclonic wind loading. *Wind and Structures*, 10(3), 269-285.
- Holmes, J. D. (1985). Wind loads and limit states design. *Civil Engineering Transactions*, Institution of Engineers Australia, CE27 (1): 21-26.
- Holmes, J.D., (2015), "Wind loading of structures", 3<sup>rd</sup> Edition, CRC Press Boca Raton, Florida, USA
- Ji, X., Huang, G., Zhang, X., & Kopp, G. A. (2018). Vulnerability analysis of steel roofing cladding: Influence of wind directionality. *Engineering Structures*, 156, 587-597.
- Lysaght (2014), "TOPSPAN Design and Installation Guide for Building Professionals", Bluescope Lysaght, Australia.
- Mahendran, M. (1994). Behaviour and design of crest-fixed profiled steel roof claddings under wind uplift. *Engineering Structures*, 16(5), 368-376.
- Parackal, K. I., Humphreys, M. T., Ginger, J. D., & Henderson, D. J. (2016). Wind Loads on Contemporary Australian Housing. *Australian Journal of Structural Engineering*, 17(2), 136-150.
- Sivapathasundaram, M., & Mahendran, M. (2016). Development of fragility curves for localised pull-through failures of thin steel roof battens. *Engineering Structures*, 124, 64-84.
- Standards Australia, (2011), "Structural design actions. Part 2 Wind actions", Australian/New Zealand Standard, AS/NZS 1170.2:2011.
- Stewart, M. G. (2016). Climate change impact assessment of metal-clad buildings subject to extreme wind loading in non-cyclonic regions. *Sustainable and Resilient Infrastructure*, 1(1-2), 32-45.
- Stewart, M. G., Ginger, J. D., Henderson, D. J., & Ryan, P. C. (2017), Fragility Analysis of Australian Contemporary Housing Roof Sheeting Failure Due to Extreme Wind. *Proceedings of 9th Asia-Pacific Conference on Wind Engineering*, Auckland, New Zealand, 3-7 Dec, 2017.